Supporting Information for

Probing Structural Flexibility of MOFs by constructing metal oxide@MOFs-based Heterostructures for Size-selective Photoelectrochemical Response

Wenwen Zhan, Yue He, Jiangbin Guo, Luning Chen, Xiangjian Kong, Haixia Zhao, Qin Kuang,* Zhaoxiong Xie, and Lansun Zheng

State Key Laboratory of Physical Chemistry of Solid Surfaces & Department of Chemistry, College of Chemistry and Chemical Engineering, Xiamen University, Xiamen, 361005, People's Republic of China

1. Experimental Section

1.1 Chemicals. Zinc acetate hydrate ($ZnAc_2 \cdot 2H_2O$, 99%), zincnitrate hexahydrate ($Zn(NO_3)_2 \cdot 6H_2O$, 99%), sodium hydroxide (NaOH, 96%), glycerine (99%), benzimidazole (99%), 4,5-dichloroimidazole (99%), imidazole (99%), N,N-dimethylformamide (DMF, 99.5%), and hexamethylenetetramine (HMTA, 99%) were purchased from commercial suppliers (Alfa Aesar and Sinopharm Chemical Regent Co., Ltd.). All chemicals were used as received without further purification.

1.2 Syntheses of samples

1.2.1 Syntheses of ZIF-7 powder for dielectric tests. $Zn(NO_3)_2 \cdot 6H_2O$ (0.575 mmol) and benzimidazole (0.423 mmol) were dissolved by 8 mL DMF, respectively. Then the two solutions were mixed together and put in a 25 mL Teflon-lined stainless-steel autoclave. After heating at 60 °C for 48 h, the white products were collected by centrifugation and washed by fresh DMF and ethanol for several times and dried by vacuum. To remove solvent of DMF, the products were alternately immersed in methanol and heated at 90 °C under vacuum for several times. The final products were saved in vacuum for dielectric measurements.

1.2.2 Syntheses of freestanding ZnO@ZIFs (ZnO@ZIF-7, ZnO@ZIF-71 and ZnO@ZIFs-zni) nanorods. Freestanding ZnO nanorods were synthesized via a hydrothermal route and then were calcined to remove the surfactants adsorbed on the nanorod surface. The growth of ZIFs on the ZnO nanorods proceeded via a simple chemical bath route. In a typical experiment, the ligand (benzimidazole, 4,5-dichloroimidazole or imidazole) and ZnO nanorods with the molar ratio of 8:1 were in sequence added to a 25 mL Teflon-lined stainless-steel autoclave containing a solvent of DMF/H_2O (15 mL, 2:1 of v/v for ZnO@ZIF-7 and ZnO@ZIF-71; 0:1 of v/v for ZnO@ZIFs-zni). After sonication for 5 min, the autoclave was transferred to a preheated oven (60 °C for ZnO@ZIF-7, 80 °C for ZnO@ZIF-71 and 85 °C for ZnO@ZIF-zni). After the mixture reacted for a specific time, the white products were

collected by centrifugation and washed by fresh DMF and ethanol for several times.

1.2.3 Syntheses of ZnO@ZIFs (ZnO@ZIF-7, ZnO@ZIF-71 and ZnO@ZIFs-zni) nanorod arrays. ZnO nanorod arrays were grown on a fluorine doped tin oxide (FTO) coated glass (2 cm × 1 cm) via a galvanostatical electrodeposition. Then the FTO glass with ZnO nanorod arrays were placed in a Teflon-lined stainless-steel autoclave containing solution of ligand (benzimidazole, 4,5-dichloroimidazole or imidazole) in a solvent of DMF/H_2O (15 mL, 2:1 of v/v for ZnO@ZIF-7 and ZnO@ZIF-71; 0:1 of v/v for ZnO@ZIFs-zni). After heating in an oven preheated to given reaction temperature (60 °C for ZnO@ZIF-7, 80 °C for ZnO@ZIF-71 and 85 °C for ZnO@ZIF-zni) for a specific time, the ZnO@ZIFs nanorod arrays were obtained and washed by ethanol and dried by vacuum.

1.3 Characterization and measurement of samples

1.3.1 Structural characterization. The compositions of the products were acquired by the powder X-ray diffraction (Rigaku Ultima IV XRD with CuKα radiation). The morphologies of the products were observed by scanning electron microscopy (SEM, S4800) and a transmission electron microscopy (TEM, TECNAI F-30) with an acceleration voltage of 300 kV, which was equipped with a Gatan image filtering (GIF) system. The thermogravimetric analysis (TGA) curves of the synthesized ZIF-7 powder were measured by using SDT Q600TGA thermal gravimetric analyzer under air atmosphere in the temperature range of 30−850 °C with a heating rate of 10 °C·min^{-1}.

1.3.2 Dielectric Tests. The data used to plot dielectric constants of ZIF-7 as functions of the temperature were collected using a Wayne Kerr 6500B impedance analyzer according to the two-probe A.C. impedance method in the frequency range of $10^{2.5}$–$10^{5.5}$ Hz. For tests, the ZIF-7 ground powder was compressed into a pellet of 5 mm in diameter with a tablet machine. After that, the tablet was coated with two silver-paste electrodes, and placed in a Janis cryogenic refrigeration system for dielectric tests.

1.3.3 Photoelectrochemical measurement. Photoelectrochemical (PEC) measurements were carried out in a three-electrode system with an electrochemical workstation (CHI 631b, Shanghai ChenhuaCo., China) under a 150 W Xenon lamp. In the PEC measurement, the FTO glasses grown with ZnO@ZIFs nanorod arrays acted as working electrode with a light intensity of 0.125 mW mm^{-2} and a light area of 8 mm^2 when working; meanwhile, a platinum wire as auxiliary electrode and saturated calomel electrode (SCE) as reference electrode. The electrolyte is consisted of standard phosphate buffer solution (pH = 6.8) and probing molecules of different concentrations. All the measurements were carried out at the voltage of 0.5 V (vs. SCE).

2. Supplementary Results

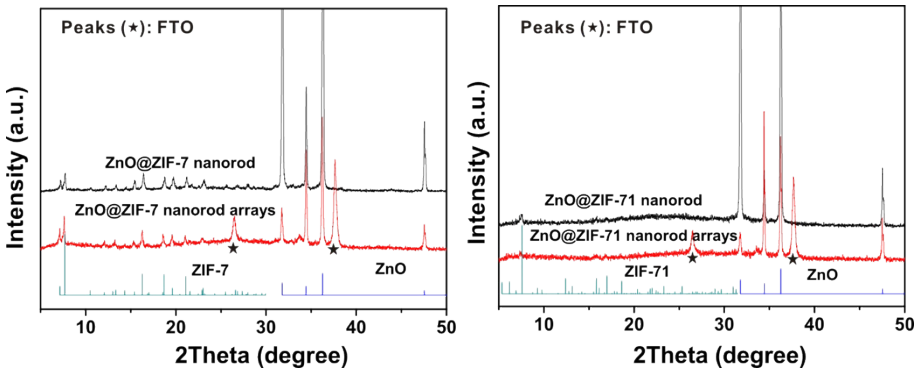

Fig. S1 XRD patterns of (a) ZnO@ZIF-7 nanorods and (b) ZnO@ZIF-71 nanorods.

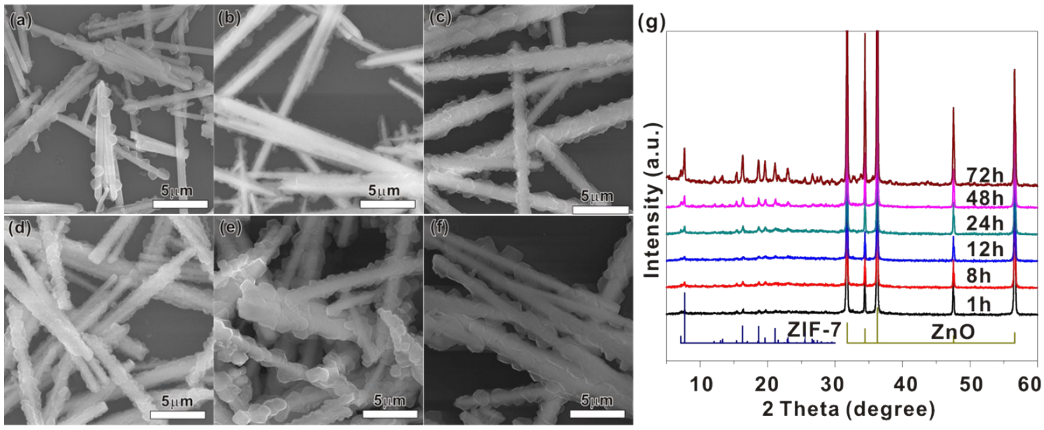

Fig. S2 (a-f) SEM images and (g) XRD patterns of the ZnO@ZIF-7 nanorods prepared with reaction time of 1, 8, 12, 24, 48, and 72h, respectively.

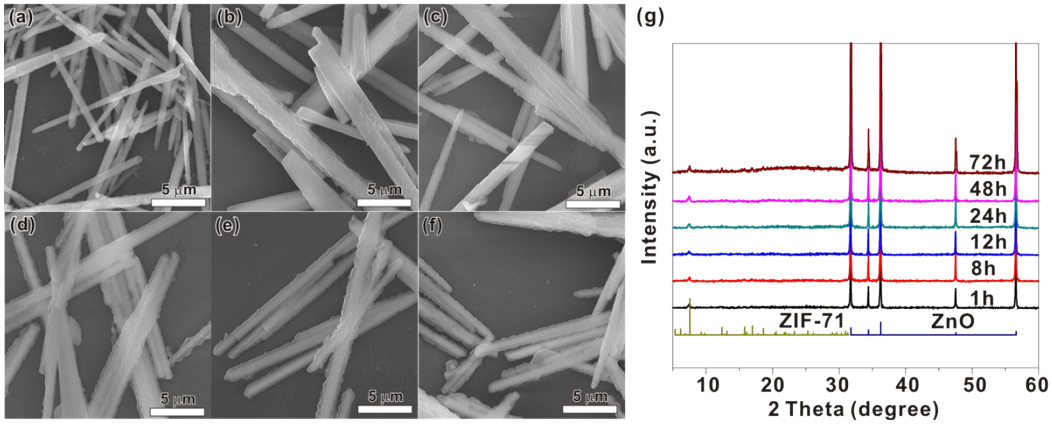

Fig. S3 (a-e) SEM images and (f) XRD patterns of the ZnO@ZIF-71 nanorods prepared with reaction time of 1, 8, 12, 24, 48, and 72h, respectively.

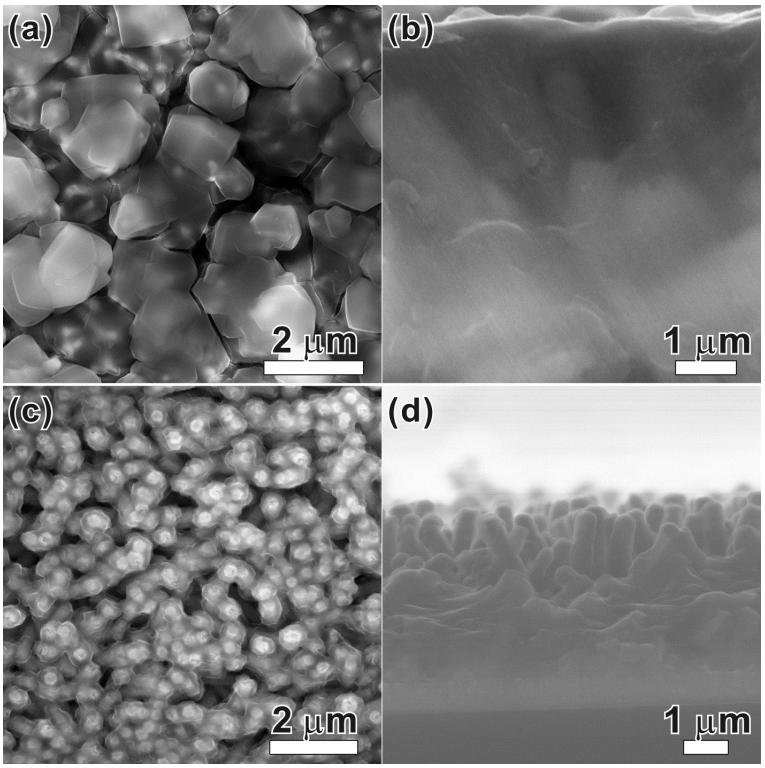

Fig. S4 SEM images of (a, b) ZnO@ZIF-7 nanorod arrays and (c, d) ZnO@ZIF-71 nanorod arrays with the top and side views, respectively.

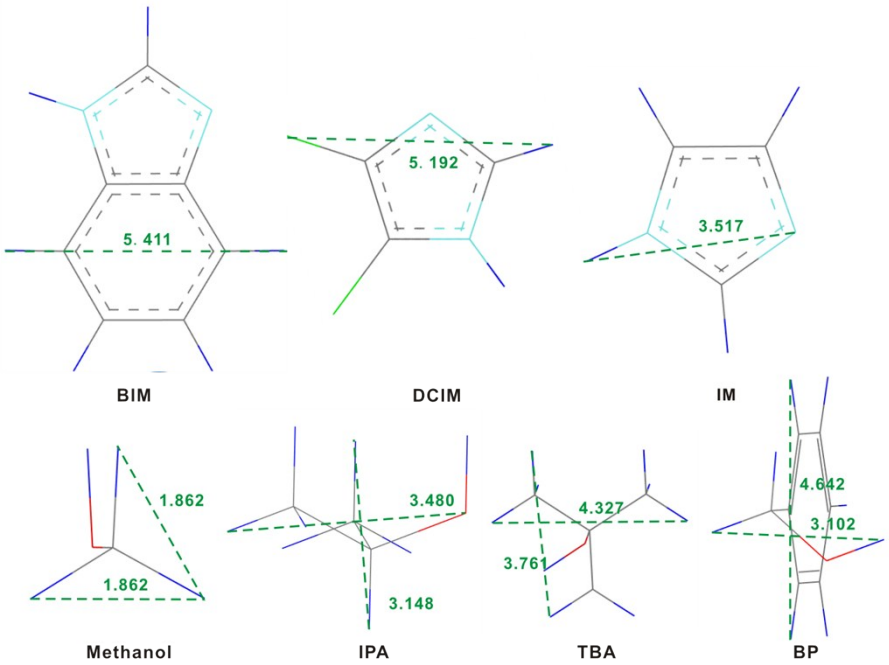

Fig. S5 The structures and sizes of ligands and four scavenger molecules.

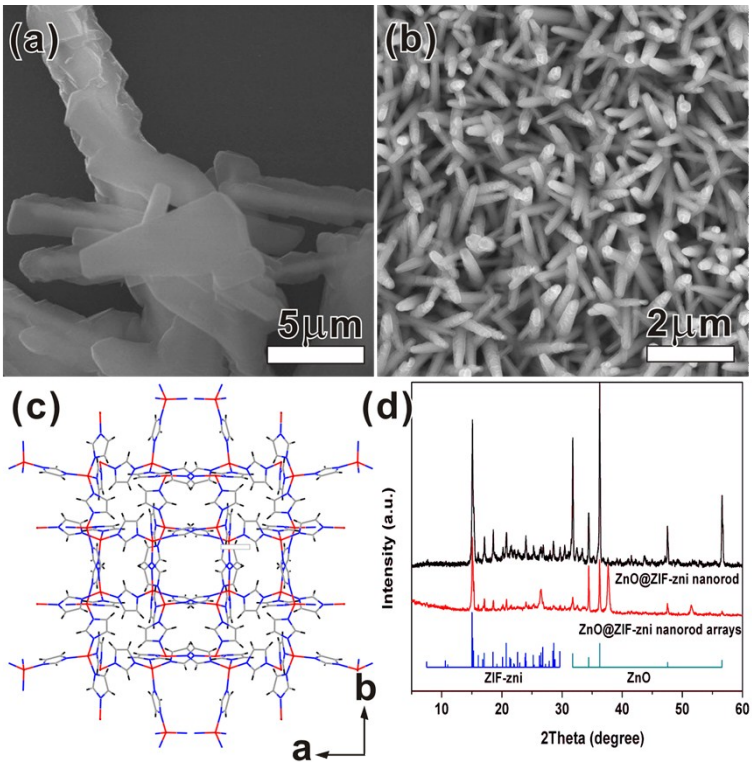

Fig. S6 SEM images of (a, b) ZnO@ZIF-zni nanorod and nanorod arrays. (c) The structure of ZIF-zni. (d) XRD patterns of ZnO@ZIF-zni nanorods and nanorod arrays.

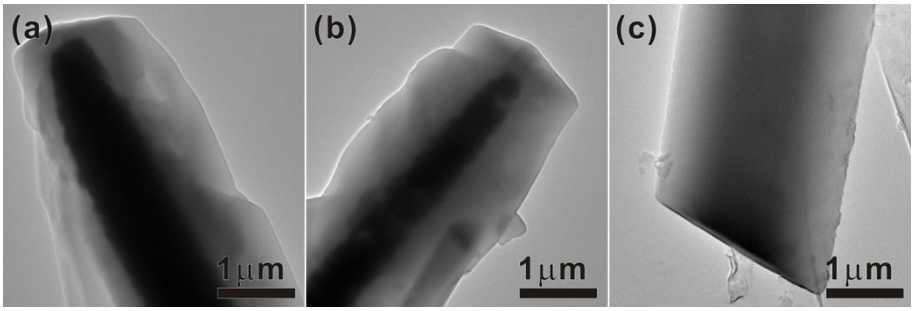

Fig. S7 (a-c) TEM images of ZnO@ZIF-zni nanorod with reaction time of 1, 8, and 24 h, respectively.

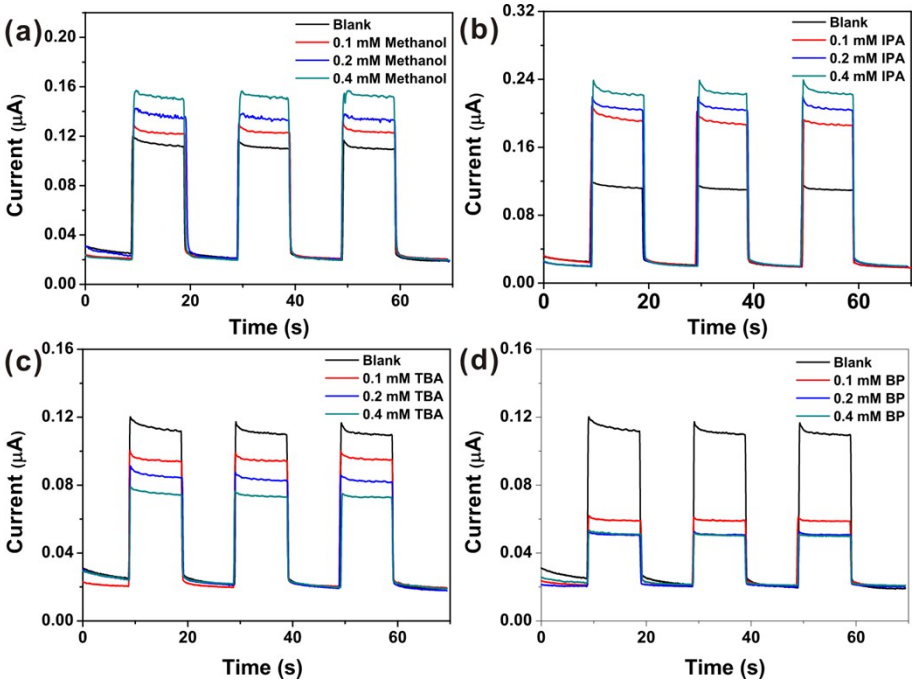

Fig. S8 Photocurrent responses of the ZnO@ZIF-71 nanorod arrays in the presence of methanol, isopropanol (IPA), tertiary butanol (TBA) and phenylcarbinol (BP) with different concentrations.

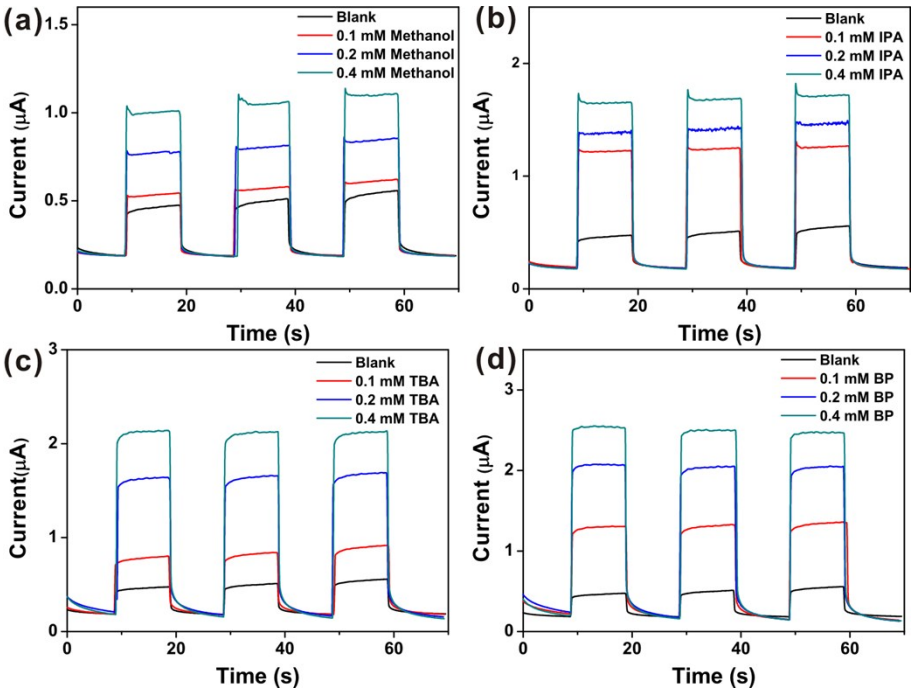

Fig. S9 Photocurrent responses of the ZnO@ZIF-7 nanorod arrays in the presence of methanol, isopropanol (IPA), tertiary butanol (TBA) and phenylcarbinol (BP) with different concentrations.

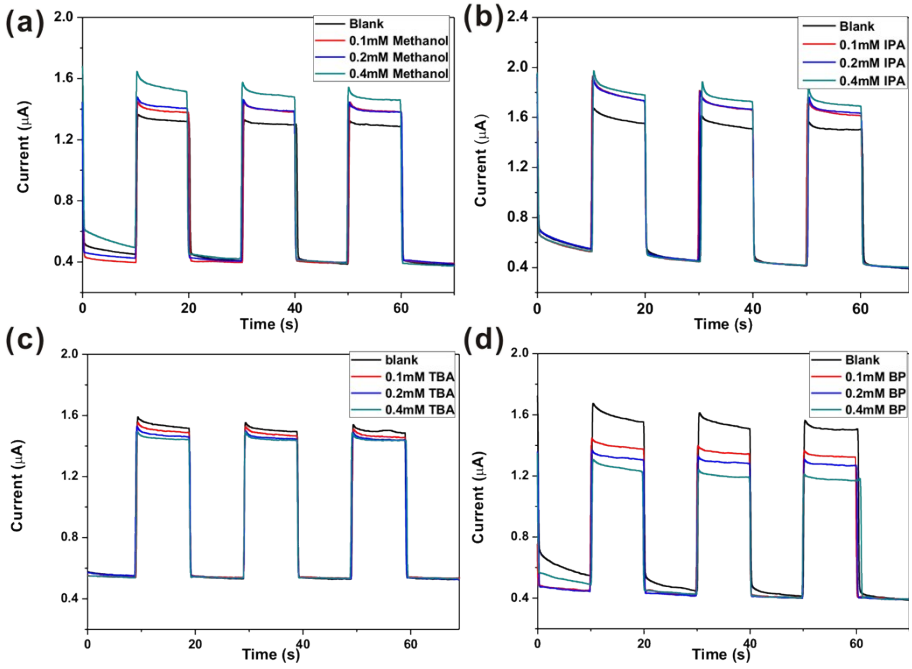

Fig. S10 Photocurrent responses of the ZnO@ZIF-zni nanorod arrays in the presence of methanol, isopropanol (IPA), tertiary butanol (TBA) and phenylcarbinol (BP) with different concentrations.

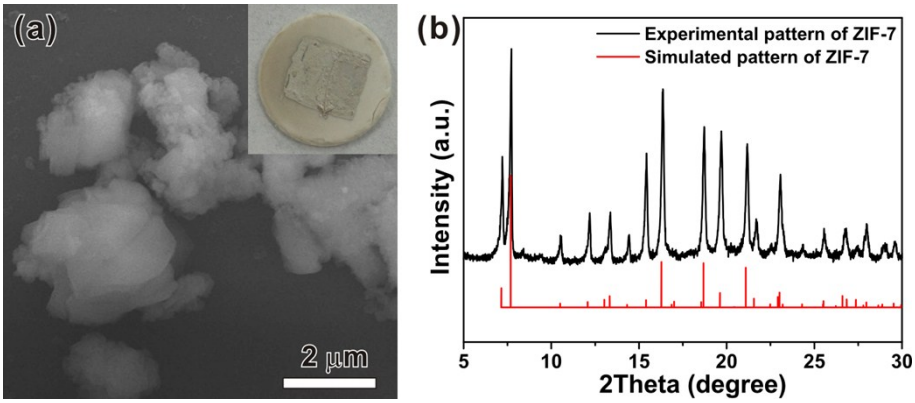

Fig. S11 (a) SEM image and (b) XRD patterns of ZIF-7 crystals before and after tableting. Inset in (a) is a photo of the ZIF-7 pellet prepared from compressed powder, which was coated with silver-paste electrodes for dielectric measurement.

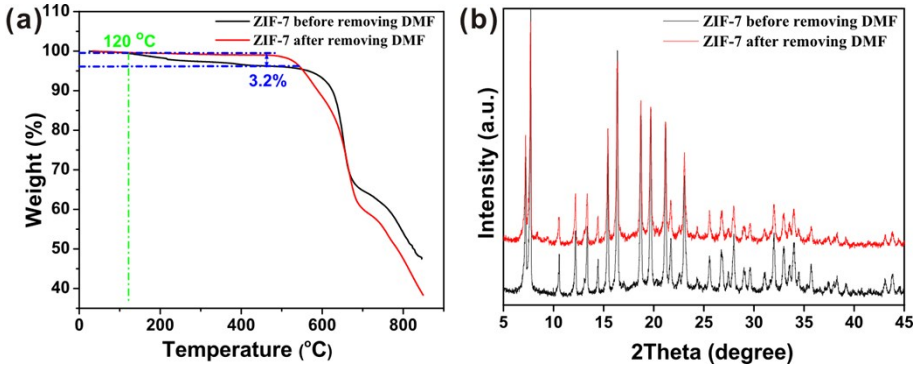

Fig. S12 (a) TGA curves and (b) XRD patterns of ZIF-7 before and after revoving DMF guest mulecules through repeated exchanging with methanol and thermal treatment under vaccum at 90 °C. (Notes: After removing DMF guest molecules, the weight loss of the ZIF-7 crystals in the range from room temperature to 500 °C was almost negligible (0.9%), which was lower by 3.2% than that of the original ZIF-7 sample. This result indicates that the DMF solvents hosted in the pores of the ZIF-7 crystals have been removed as completely as possible. The XRD patterns further revealed that the DMF-removing treatment didn't cause damage to the structure of ZIF7.)

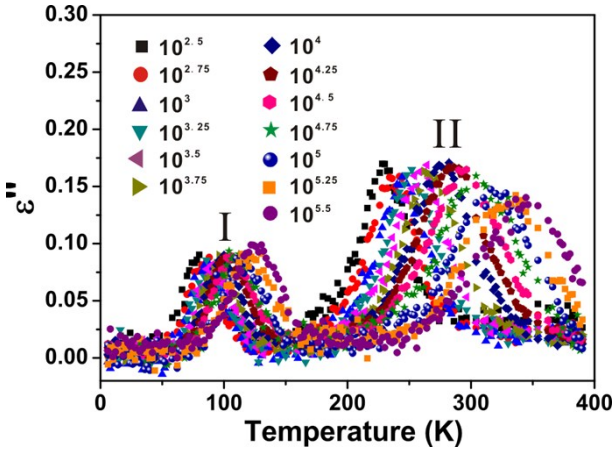

Fig. S13. Imaginary parts (ε'') of the complex dielectric constants at various frequencies and temperatures for ZIF-7 with DMF molecules hosted in the pores.

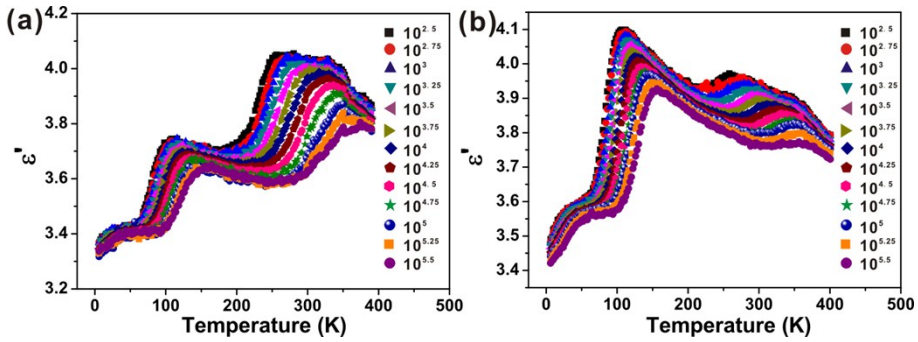

Fig. S14. Real parts (ε') of the complex dielectric constants at various frequencies and temperatures for ZIF-7 (a) before and (b) after removing DMF molecules.